HHS Public Access

Author manuscript

Neuroscience. Author manuscript; available in PMC 2017 January 02.

Published in final edited form as:

Neuroscience. 2010 November 10; 170(4): 1065–1079. doi:10.1016/j.neuroscience.2010.07.064.

DISTRIBUTION AND NEUROCHEMICAL CHARACTERIZATION OF PROTEIN KINASE C-THETA AND -DELTA IN THE RODENT HYPOTHALAMUS

B. G. IRANI[a], **J. DONATO JR**[a], **D. P. OLSON**[b], **B. B. LOWELL**[b], **T. C. SACKTOR**[c], **M. E. REYLAND**[d], **K. P. TOLSON**[e], **A. R. ZINN**[e], **Y. UETA**[f], **I. SAKATA**[a], **J. M. ZIGMAN**[a], **C. F. ELIAS**[a], and **D. J. CLEGG**[a,*]

[a]Department of Internal Medicine, University of Texas Southwestern Medical Center, 5323 Harry Hines Boulevard, Dallas, TX 75390-8854, USA

[b]Department of Medicine, Division of Endocrinology, Beth Israel Deaconess Medical Center and Harvard Medical School, Boston, MA 02215, USA

[c]The Robert F. Furchgott Center for Neural and Behavioral Science, Departments of Physiology, Pharmacology, and Neurology, SUNY Downstate Medical Center, 450 Clarkson Avenue, Brooklyn, NY 11203, USA

[d]Department of Craniofacial Biology, University of Colorado Denver, Anschutz Medical Campus, Aurora, CO 80045, USA

[e]McDermott Center for Human Growth and Development, The University of Texas Southwestern Medical Center, 5323 Harry Hines Boulevard, Dallas, TX 75390-8591, USA

[f]Department of Physiology, School of Medicine, University of Occupational and Environmental Health, Kitakyushu 807-8555, Japan

Abstract

PKC-theta (PKC-θ), a member of the novel protein kinase C family (nPKC), regulates a wide variety of functions in the periphery. However, its presence and role in the CNS has remained largely unknown. Recently, we demonstrated the presence of PKC-θ in the arcuate hypothalamic nucleus (ARC) and knockdown of PKC-θ from the ARC protected mice from developing diet-induced obesity. Another isoform of the nPKC group, PKC-delta (PKC-δ), is expressed in several non-hypothalamic brain sites including the thalamus and hippocampus. Although PKC-δ has been implicated in regulating hypothalamic glucose homeostasis, its distribution in the hypothalamus has not previously been described. In the current study, we used immunohistochemistry to examine the distribution of PKC-θ and -δ immunoreactivity in rat and mouse hypothalamus. We found PKC-θ immunoreactive neurons in several hypothalamic nuclei including the ARC, lateral hypothalamic area, perifornical area and tuberomammillary nucleus. PKC-δ immunoreactive neurons were found in the paraventricular and supraoptic nuclei. Double-label immunohistochemisty in mice expressing green fluorescent protein either with the long form of leptin receptor (LepR-b) or in orexin (ORX) neurons indicated that PKC-θ is highly colocalized in

*Corresponding author. Tel: +1-214-648-3401; fax: +1-214-648-8720. deborah.clegg@utsouthwestern.edu (D. J. Clegg).

lateral hypothalamic ORX neurons but not in lateral hypothalamic LepR-b neurons. Double-label immunohistochemistry in oxytocin-enhanced yellow fluorescent protein mice or arginine vasopressin-enhanced green fluorescent protein (AVP-EGFP) transgenic rats revealed a high degree of colocalization of PKC-δ within paraventricular and supraoptic oxytocin neurons but not the vasopressinergic neurons. We conclude that PKC-θ and -δ are expressed in different hypothalamic neuronal populations.

Keywords

feeding; orexin; oxytocin; lateral hypothalamic area; glutamate; arousal

Protein kinase C (PKC) comprises a group of serine/threonine kinases which play an important role in regulating a broad spectrum of neuronal activities including neuronal differentiation (Campenot et al., 1994), modulation of ion channels (Shearman et al., 1989), desensitization of receptors (Huganir and Greengard, 1990) and glutamate-induced neurotoxicity (Felipo et al., 1993). One class of PKCs, called the novel PKC (nPKC) includes PKC-δ, ε, η and θ. These PKCs exhibit enzymatic activity in the presence of phosphatidylserine (PS) and diacylglycerol (DAG), but are independent of intracellular calcium (Ca^{2+}) levels (Ono et al., 1988; Konno et al., 1989). PKC-δ and ε isoforms have previously been demonstrated to be widely distributed in several regions of the CNS (Wetsel et al., 1992; Saito et al., 1993; Tanaka and Nishizuka, 1994). In contrast, early reports suggested PKC-θ was mainly expressed in peripheral tissues such as skeletal muscle (Osada et al., 1992), and not in the rodent brain (Tanaka and Nishizuka, 1994). Nearly a decade later, Minami and colleagues detected PKC-θ expression in the habenula of the rat brain (Minami et al., 2000). However, using *in situ* hybridization, they did not observe hypothalamic expression of PKC-θ. Additionally, PKC-δ immunoreactivity, while present in the brain, was also not previously observed in hypothalamic nuclei (Merchenthaler et al., 1993; Naik et al., 2000).

Recently, we and others demonstrated expression of PKC-θ (Dewing et al., 2008) and its immunoreactivity (Benoit et al., 2009) in the arcuate hypothalamic nucleus (ARC). The ARC is a key CNS site known to regulate food intake (Schwartz et al., 2000), glucose homeostasis (Anand et al., 1964), reproduction (Hill et al., 2008) and arousal (Yamanaka et al., 2003; Adamantidis and de Lecea, 2008). The ARC contains two neuronal populations with opposing actions, the anorexigenic proopiomelanocortin (POMC) neurons and the orexigenic neuropeptide Y/agouti-related protein (NPY/AgRP) neurons. Both of these express the long form of the leptin receptor (LepR-b) (Mercer et al., 1996; Cheung et al., 1997) as well as the insulin receptor (Marks et al., 1990; Niswender and Schwartz, 2003). ARC POMC neurons are activated by insulin and leptin (Cowley et al., 2001) and secrete the anorexic neuropeptide, α-melanocyte stimulating hormone (α-MSH). Orexigenic neurons expressing NPY/AgRP are inhibited by insulin and leptin (Niswender and Schwartz, 2003; van den Top et al., 2004). ARC neurons expressing α-MSH and AgRP innervate the melanin-concentrating hormone (MCH) and orexin (ORX) neurons in the perifornical region and lateral hypothalamic area (LHA) (Broberger et al., 1998; Elias et al., 1998), areas also important for the regulation of food intake and body weight (Anand and Brobeck, 1951). We

recently demonstrated that ARC-specific knockdown of PKC-θ attenuated diet-induced obesity and improved insulin signaling (Benoit et al., 2009). Additionally, Ross and colleagues have implicated hypothalamic PKC-δ in mediating glucose production (Ross et al., 2008). Hence, activation of nPKCs may play a crucial role in regulating hypothalamic neuroendocrine functions.

While previous studies have described PKC-θ and -δ distribution in rodent brains, these studies were not focused on the hypothalamus. Here we systematically determined the distribution of PKC-θ and -δ immunoreactivity in the basal medial hypothalamus of rat and mouse brains and, we used double-label immunohistochemistry with green fluorescent protein (GFP) or enhanced yellow fluorescent protein (EYFP) neuronal-specific reporter mice and/or rats to investigate the neurochemical identity of PKC-θ and -δ hypothalamic neurons. Information on the distribution and co-localization with other key neuroendocrine cells will be valuable for identifying the role and function of PKC-θ and -δ in mediating metabolic functions.

EXPERIMENTAL PROCEDURES

Animals

Adult, male, Long-Evans rats (250–300 g, *n*=5; Harlan) and C57BL/6 mice (25–30 g, 14 wk old, *n*=5; Jackson Laboratories) were housed with *ad libitum* access to food and water in a light-(12 hours on/12 hours off) and temperature-(22–23 °C) controlled environment. The LepR-b-EGFP mice (*n*=3) were provided by Dr. Martin Myers Jr (University of Michigan, Ann Arbor, MI, USA); orexin-GFP mice (*n*=3) were provided by Dr. Masashi Yanagisawa (UT Southwestern Medical Center, Dallas, TX, USA); arginine vasopressin-enhanced green fluorescent protein (AVP-EGFP) transgenic rats (*n*=3) and oxytocin-EYFP (Oxt-EYFP) mice (*n*=3) were provided by Dr. Andrew Zinn (UT Southwestern Medical Center, Dallas, TX, USA). The animals and procedures used for these studies were in accordance with the UT Southwestern Institutional Animal Care and Use Committee.

Generation of transgenic mice

The generation of the LepRb-EGFP mice has been described previously (Leinninger et al., 2009). Briefly, the LepR-Cre mice were crossed with Gt(Rosa)-26-Sor^{tm2Sho} (Jackson Laboratory) and the double heterozygous progeny were intercrossed to generate LepR-Cre/Cre; Gt(Rosa)-26-Sor$^{tm2Sho/tm2Sho}$ (i.e., LepR-b-EGFP) mice (Leshan et al., 2009). The generation of the ORX-GFP mouse has been described previously (Li et al., 2002). The Lac Z gene under control of a human hypocretin promoter was used to drive the GFP sequence (Sakurai et al., 1999). The generation of the PKC-δ KO mice has been described previously (Miyamoto et al., 2002). The target vector was constructed by replacing a 2.8-kb HpaI-BamH1 fragment containing exons I and II of the PKC-δ gene with a phosphoglycerate kinase (PGK)-neo-poly(A) cassette. Mutant embryonic stems cells were prepared and microinjected into C57BL/6 blastocysts, and the resulting male chimeras were mated with female C57BL/6 mice. Heterozygous breeding strategy was used to produce homozygous PKC-δ KO mice. The validity of the above three transgenic mouse models has been verified previously (Li et al., 2002; Miyamoto et al., 2002; Yamanaka et al., 2003; Humphries et al.,

2006; Leinninger et al., 2009; Leshan et al., 2009). The generation and validation of the AVP-EGFP transgenic rats has been described previously (Ueta et al., 2005).

The *Oxt*-Cre transgenic mice were generated by using methods described previously (Lee et al., 2001; Balthasar et al., 2005). Briefly, Cre recombinase and a polyadenylation signal were targeted to the initiator methionine codon of the Oxt gene using recombineering techniques with bacterial artificial chromosome (RP24-388N9) (Lee et al., 2001; Balthasar et al., 2005). A fragment of genomic DNA containing the targeted *Oxt* gene plus 10 kb of upstream flanking sequence (Fig. 1A) and the downstream vasopressin gene lacking its initiator codon and upstream sequences was subcloned (Fig. 1B). The resulting construct was injected into pronuclei of fertilized mouse oocytes, and a transgenic line expressing Cre recombinase in the hypothalamus was obtained. Finally, this line was crossed with Rosa26-EYFP reporter mice (Jackson Laboratory, stock number 006148) to generate the Oxt-EYFP mice. We confirmed the validity of this mouse model by carrying out double label immunofluorescence for oxytocin (Fig. 1C) and EYFP (Fig. 1D). Majority of cells that expressed EYFP were also positive for oxytocin immunoreactivity (Fig. 1E). Few oxytocin immunoreactive neurons showed relatively little EYFP expression suggesting that not every oxytocin neuron expresses detectable EYFP (Fig. 1E).

Histology

Rats and mice were deeply anesthetized with an intraperitoneal injection of chloral hydrate (7%; 350 mg/kg; Sigma, St. Louis, MO, USA) and perfused transcardially with DEPC-treated 0.9% saline followed by 4% paraformaldehyde or 10% neutral buffered formalin. Brains were removed, post-fixed in 10% formalin for 2 h and then transferred to 20% sucrose made in DEPC-treated phosphate-buffered saline (PBS), pH 7.0 at 4 °C. Brains were cut coronally at 40 μm (for rats) or 25 μm (for mice) into five equal series on a freezing microtome. Tissue was stored at −20 °C in antifreeze solution until processed for immunohistochemistry.

Preparation and specificity of primary antibodies

The PKC-θ antiserum was purchased from Santa Cruz Biotechnology (catalog no. sc-212, lot no. L2408, Santa Cruz, CA, USA). The PKC-θ antiserum is a rabbit polyclonal affinity purified antibody raised against a peptide mapping at the C-terminus of the PKC-θ of mouse origin. Previously, we confirmed the specificity of the antibody in tissue from PKC-θ KO mice (Benoit et al., 2009). We did not observe any staining in the hypothalamic sections of PKC-θ KO mice.

The PKC-δ antiserum was provided by Dr. Todd Sacktor, SUNY Downstate Medical Center, NY, USA. The preparation of the rabbit polyclonal antibody has been described previously (Naik et al., 2000). The antiserum was prepared against a synthetic peptide consisting of a NH_2-terminal cysteine followed by the sequence of the carboxyl-terminal variable region for PKC-δ: NPKYEQFLE. No staining was observed when the primary antibody was preincubated with 2 μg/mL of the immunizing peptide. We further confirmed the specificity of this antiserum in PKC-δ KO mice.

The guinea pig anti-histidine decarboxylase antibody was purchased from Alpco Diagnostics (catalog no. B-GP- 265-1, lot no. HS-4061, Salem, NH, USA) (Zhao et al., 2008a). The chicken anti-GFP antibody was purchased from Aves Lab Inc. (catalog no. GFP-1020, lot no. 1223FP03, Aves Labs Inc., Tigard, OR, USA) and its specificity has been previously confirmed (Zhao et al., 2008b). Chickens were immunized with fluorescent GFP, eggs were collected from hens after multiple injections and IgY fractions were prepared from the yolks. The manufacturer has confirmed the specificity of the antibody by western blot analysis and immunohistochemistry in transgenic mice expressing the GFP product.

Immunohistochemistry (IHC)

Rats—For each animal, a series of sections extending from the anterior olfactory nucleus to the caudal end of the ARC was subjected to a standard immunoperoxidase reaction. Sections were pretreated with 0.3% hydrogen peroxide, after which they were blocked with 3% normal donkey serum (Jackson Laboratories, West Grove, PA, USA) and 0.3% Triton X-100 (Sigma, St. Louis, MO, USA). Subsequently, sections were incubated in 1:2000 PKC-θ (catalog no. sc-212, Santa Cruz Biotechnology, CA, USA) or 1:2000 PKC-δ (Naik et al., 2000) rabbit primary anti sera overnight at room temperature. Sections were then incubated for 1 h in biotin-conjugated IgG donkey anti-rabbit (1:1000, Jackson Laboratories) and for 1 h in avidin–biotin complex (1:500, Vector Labs, Burlingame, USA). The sections were then submitted to a 4–6 min immunoperoxidase reaction with 0.03% hydrogen peroxide using diaminobenzidine tetrahydrochloride (DAB; catalog no. D5905; Sigma) as the chromogen. The reaction was terminated with rinses in PBS. Sections were mounted onto gelatin-coated slides, dehydrated, delipidated and coverslipped with DPX (Fluka; Sigma-Aldrich Chemie GmbH, Deisenhofen, Germany).

An adjacent series of sections was thionin stained to identify PKC-positive nuclear cell bodies. Briefly, the sections were mounted on gelatin-coated slides and dried overnight at room temperature. On the following day, sections were dehydrated in ethyl alcohol and cleared in xylene for 30 min. The slides were gradually rehydrated in ethanol solution and immersed in a 0.25% thionin solution for 1 min. The sections were rinsed in water, dehydrated in graded ethanols and dipped in xylene, and then slides were cover-slipped with DPX (Fluka; Sigma-Aldrich).

Mice—Both, single- and double-label immunofluorescence were performed. First, to identify brain nuclei expressing either PKC-θ or PKC-δ, we performed single-label IHC. Adjacent coronal series of sections extending from the anterior olfactory nucleus to the caudal end of the NTS were pretreated with hydrogen peroxide, incubated for 30 min in 3% normal donkey serum (Jackson ImmunoResearch Laboratories, West Grove, PA, USA) with 0.25% Triton X-100 in PBS (PBT) with 0.02% sodium azide. Sections were incubated overnight at room temperature in 1:200 PKC-θ (catalog no. sc-212, Santa Cruz Biotechnology, CA, USA) or 1:500 PKC-δ rabbit primary antisera (Naik et al., 2000). After washing in PBS, tissue was incubated in fluorescently labeled Alexa 594 or Alexa 488 donkey secondary antisera (Invitrogen, Carlsbad, CA, USA) diluted to 1:200 in PBT for 1 h at room temperature. Tissues were then rinsed in PBS and mounted on gelatin coated slides.

Dried slides were cover-slipped using Fluoromount G (catalog no. 17984-25, Electron Microscopy Sciences, Hatfield, PA, USA).

For double label IHC for EYFP and Oxt labeling, coronal brain sections were permeabilized and blocked in 3% normal goat serum/0.3% Triton X-100 for 1 h, and incubated for 48 h at 4 °C in 1:5000 rabbit anti-GFP antiserum (catalog no. A6455, Molecular Probes, Eugene, OR, USA) and 1:5000 mouse anti-Oxt antiserum (catalog no. MAB5296, Millipore Corp., Billerica, MA, USA). Sections were then incubated with fluorescein isothiocyanate goat antirabbit IgG secondary antiserum and 1:400 Cy-2 affiniPure goat antimouse IgG secondary antiserum (catalog no.115-225-166, Jackson ImmunoResearch) for 2 h at room temperature. Sections were placed in 0.2 μg/mL 4′,6-diamidino-2-phenylindole (catalog no. 236276; Roche, Indianapolis, IN, USA) for 10 min and then mounted on plus coated slides and coverslipped using Vectashield (catalog no. H-1000; Vector Laboratories, Burlingame, CA, USA). Images of sections containing paraventricular hypothalamic nucleus (PVN) were captured on an Olympus BX61 microscope using Cytovision software (Applied Imaging Corp., San Jose, CA, USA).

The sections from LepR-b-EGFP, C57BL/6 mice (n=3) and ORX-GFP (n=3) were incubated in PKC-θ antisera. Sections from oxytocin-EYFP mice (n=3) and AVP-EGFP rats (n=3) were incubated in PKC-δ antisera and then processed as described above. Sections from LepR-b-EGFP, ORX-GFP, oxytocin-EYFP mice and AVP-EGFP rats were washed in PBS, and then incubated in 1:5000 chicken, anti-GFP antibody (catalog no. GFP-1020, Aves Labs Inc., Tigard, OR, USA).

For PKC-θ/GFP and PKC-δ/YFP double-label IHC, sections were then washed in PBS, and the tissue was incubated in fluorescently labeled Alexa 488 donkey secondary antisera (Invitrogen) diluted to 1:200 in PBT for 1 h at room temperature. For the PKC-θ/histidine decarboxylase (HDC) double-label IHC brain sections were incubated in 3% normal goat serum/0.3% Triton X-100 for 1 h, and incubated for 48 h at 4 °C in 1:5000 anti-HDC antiserum (ALPCO Diagnostics) and 1:200 anti-PKC-θ antiserum. Sections were then incubated Alexa 488 donkey anti-rabbit IgG and Alexa 594 goat anti-guinea pig IgG secondary antisera (invtrogen), diluted 1:200 respectively, for 2 h at room temperature. Tissues were then rinsed in PBS and mounted on gelatin coated slides. Dried slides were cover-slipped using Fluoromount G (catalog no. 17984-25, Electron Microscopy Sciences, Hatfield, PA, USA).

Production of photomicrographs

Sections were analyzed using a Zeiss Axioplan light microscope and Zeiss Apotome microscope. Adobe Photoshop CS2 9.0 (Adobe Systems, San Jose, CA, USA) was used to adjust only sharpness, brightness and contrast as well as to combine select images into plates. Unless otherwise noted, nomenclature corresponds to the Paxinos and Franklin (2001, 2nd Edition) mouse brain atlas.

Cell counts and data analysis

Single and double-labeled cells were counted in brain regions demonstrating colocalization of PKC-θ and orexin. PKC-θ and orexin cells were counted in the LHA, perifornical area

(Pfx) and ventral part of dorsomedial hypothalamic nucleus DMN (vDMN). Cells were counted from the same atlas level for all three nuclei (Paxinos and Franklin, 2001, 2nd Edition). Similarly, PKC-δ and oxytocin cells were counted in the PVN and supraoptic nucleus (SON) from the same atlas level. Cells were counted from three separate mice (n=3) and counts are presented as mean±SEM. These data were corrected for double counting by applying Abercombie's formula, N=n(T/T+D), where N=corrected cell count, n=observed number of cells, T=section thickness (25 μm) and D=diameter of nucleus (Guillery and Herrup, 1997). For each brain area with double-labeled cells we calculated the mean nuclear diameter from 10–12 random cells. We did not use stereological techniques for cell count estimation.

RESULTS

Distribution of PKC-θ immunoreactivity in rat brain

PKC-θ immunoreactive (IR) neurons were observed in discrete regions of the CNS. In the thalamus (Fig. 2A, B), the highest concentration of PKC-θ-IR cells was in the medial habenular nucleus (MHb), and a few PKC-θ-IR cells were observed ventral to the MHb in the paraventricular thalamic nucleus (PVT) and lateral habenular nucleus (LHb). In the hypothalamus, the highest concentration of PKC-θ-IR neurons were at the tuberal level dorsal to the fornix in a region that comprises the LHA and zona incerta (Fig. 2C, D). A few PKC-θ-IR neurons were observed in the vDMN (Fig. 2E). We confirmed our previous findings (Benoit et al., 2009) demonstrating PKC-θ-IR neurons in the tuberal level of the ARC (Fig. 3A), and also found cells in the posterior level of the ARC (Fig. 3B).

Distribution of PKC-δ immunoreactivity in rat brain

We confirmed the presence of PKC-δ-IR neurons in the thalamus, septal nuclei and hippocampus (Merchenthaler et al., 1993; Naik et al., 2000). Although, PKC-δ-IR neurons are found in several thalamic nuclei, the highest concentrations were in the ventral posterolateral (VPL) and ventral posteromedial (VPM) thalamic nuclei (Fig. 4A, B). PKC-δ-IR was also found in the hypothalamus where its distribution was limited to the PVN (Fig. 4C) and SON (Fig. 4D). Consistent with previous findings, our data suggest PKC-δ immunoreactivity is primarily neuronal (Merchenthaler et al., 1993; Naik et al., 2000).

Distribution of PKC-θ immunoreactivity in mouse brain

Fluorescent IHC demonstrated a similar distribution of PKC-θ-IR neurons in the mouse brain (Table 1). High concentrations of PKC-θ-IR neurons in the mouse were observed in the MHb, LHA, Pfx and tuberomammillary nucleus. Similar to the rat, PKC-θ-IR neurons were also observed in the ARC and vDMN.

Fibers from PKC-θ-IR-positive neurons were found throughout the mouse brain (Table 1). A few immunoreactive fibers were observed in the piriform cortex and primary somatosensory cortex; moderate-density immunoreactive fibers were found in the medial preoptic nucleus, medial forebrain bundle, periventricular area, lateral septal nucleus, ventromedial hypothalamic nucleus (VMN), ARC, posterior hypothalamic area (PH), supramammillary nucleus (SuM), and medial mamillary nucleus (MM); and dense innervation was observed in

the anterior hypothalamic area (AHA) and PVN. Moderate density of PKC-θ-IR fibers was observed in both the anterior and posterior portions of the PVT (Table 1).

In the midbrain, a high density of PKC-θ-IR fibers was observed in the ventral tegmental area (VTA), while a moderate density was observed in the interpenduncular nucleus, substantia nigra (SN), dorsal raphe (DR) and periaqueductal gray (PAG). In addition, we found a few fibers in the nucleus of the solitary tract (NTS), hypoglossal nucleus (12 N), lateral reticular nucleus (LRt), and the ventral part of medullary reticular nucleus (MdV).

Distribution of PKC-δ immunoreactivity in mouse brain

As indicated in Table 1, PKC-δ-IR neurons were observed in several thalamic nuclei, with the densest immunoreactivity in the reticular thalamic nucleus (Rt), VPM and VPL (Fig. 5A, B). No staining for PKC-δ was found in these thalamic nuclei in PKC-δ KO mice (Fig. 5C), thus validating the specificity of the antibody. Similar to the rat, there were moderate density PKC-δ-IR neurons in the LS and CA3 field, and few PKC-δ-IR neurons were observed in the dentate gyrus and CA1 field (Table 1).

In the hypothalamus, there was a high concentration of PKC-δ-IR neurons in the PVN, SON and dorsal portion of the suprachiasmatic nucleus (SCh). We also observed a few PKC-δ-IR neurons in the AHA region between the PVN and SON. In the amygdala, a higher concentration of PKC-δ-IR neurons was in the dorsal part of the anterior amydaloid area (AAD) than in the ventral portion.

In comparison to PKC-θ-IR fibers, the distribution of PKC-δ-IR fibers was very limited in the mouse brain. Specifically, PKC-δ-dense immunoreactive fibers were found in the ME and SCh, while moderate density fibers were observed in the periventricular area and LS (Table 1).

Neurochemical characterization of hypothalamic PKC-θ expressing cells

We also determined the neurochemical identity of the hypothalamic PKC-θ-IR neurons. We had previously demonstrated 20% colocalization of PKC-θ with ARC NPY neurons (but not POMC neurons) and ~22% colocalization of PKC-θ with LepR-b in the ARC (Benoit et al., 2009). LepR-b neurons have also been demonstrated in the Pfx and LHA of mouse brain (Leinninger et al., 2009; Scott et al., 2009), and, we found no colocalization of GFP-IR and PKC-θ-IR in the Pfx or LHA (Fig. 6A–C) of LepRb-EGFP mice.

Orexin neurons are exclusively found in the Pfx and LHA of the mouse brain and have no colocalization with LepR-b neurons in the LHA (Li et al., 2002; Leinninger et al., 2009). Double-label IHC for ORX-GFP and PKC-θ-IR (Fig. 7A–C) revealed a high percentage of colocalization in the Pfx (86.7±1.9% of total PKC-θ-IR neurons) and LHA (82.8±8.6% of total PKC-θ-IR neurons) (Table 2). PKC-θ immunoreactive fibers were also observed in the PVN and VTA (Table 1), which are also known to receive dense innervation from ORX fibers (Fig. 7D–I) (Date et al., 1999; Nambu et al., 1999). We also observed a high degree of PKC-θ and ORX-immunoreactive fibers in the PVN (Fig. 7D–F) and VTA (Fig. 7G–I). Apparent appositions of PKC-θ and ORX immunoreactive fibers were observed in both the PVN (Fig. 7F) and VTA (Fig. 7I); however, overlapping fiber distribution was only observed

in the PVN (Fig. 7F). We also observed apparent innervations of histamine neurons by PKC-θ immunoreactive fibers in the ventral tuberomammillary nucleus (VTM) (Fig. 8A–C).

Neurochemical characterization of hypothalamic PKC-δ expressing cells

Double-label IHC for GFP-like immunoreactivity (Fig. 9A, B) and PKC-δ-IR in Oxt-EYFP mice revealed a high degree of colocalization of PKC-δ-IR and GFP-IR in PVN (Fig. 9C–E) and SON (Fig. 9F–H) neurons. In the PVN, 83.4±2.9% of PKC-δ-IR neurons were colocalized with Oxt neurons while in the SON 84.5±5.3% had colocalization (Table 3). Although, results from double label IHC for PKC-δ and YFP immunoreactivity in oxytocin-EYFP mice (Fig. 1C–E) might not necessarily represent the accurate number of colocalized neurons we next determined whether the ~15% non-oxytocin-PKC-δ neurons are AVP neurons. We did not observe any colocalization of PKC-δ-IR neurons with AVP neurons in either the PVN (Fig. 10A–C) or the SCh (Fig. 10D–F) suggesting that PKC-δ neurons in these two regions of the mouse hypothalamus are mainly oxytocin neurons.

DISCUSSION

We have characterized the distribution and neurochemical identity of PKC-θ and PKC-δ neurons in the CNS, focusing on the hypothalamus. Our findings suggest that PKC-θ and PKC-δ neurons have distinct distribution patterns in the rat and mouse brain. We replicated previous findings demonstrating the presence of PKC-θ immunoreactivity in the ARC of the mouse and rat (Benoit et al., 2009) and PKC-δ immunoreactivity in the septal nuclei, thalamus and hippocampus of the rat brain (Merchenthaler et al., 1993; Naik et al., 2000). Additionally, we have demonstrated the presence of PKC-θ immunoreactivity in the LHA and tuberomamillary nucleus of the hypothalamus, whereas PKC-δ immunoreactivity was found predominately in the PVN and SON. Finally, we found that PKC-θ is highly colocalized with orexin neurons in the Pfx and LHA, while PKC-δ is highly colocalized with oxytocin neurons in the PVN and SON.

Comparison of PKC-θ versus PKC-δ distribution

As indicated in Table 1, the distribution patterns of cell bodies containing PKC-θ and PKC-δ were distinct. In the thalamus, PKC-θ immunoreactive neurons were mainly restricted to the MHb and PVT, while PKC-δ cell bodies were extensively distributed in several thalamic nuclei with high concentrations in the VPL and VPM. In opposition, we observed a high number of PKC-θ immunoreactive neurons in the perifornical area, LHA, and tuberomamillary nucleus of the hypothalamus, while PKC-δ immunoreactive neurons were mainly limited to the PVN and SON.

Functional implications: PKC-θ in orexin neurons

For the first time, we have demonstrated a high degree of colocalization of PKC-θ in orexin neurons, suggesting that PKC-θ may be an important downstream mediator of orexin activity, which has been implicated in feeding and arousal (Sakurai et al., 1998; Yamanaka et al., 2000; Tsujino and Sakurai, 2009).

Feeding—A critical role has been identified for LHA orexin neurons in feeding and energy homeostasis (Sakurai et al., 1998; Yamada et al., 2000; Yamanaka et al., 2000). Central administration of an anti-orexin antibody or orexin receptor 1 (OX1R)-selective antagonist reduces food intake in rats (Haynes et al., 2000; Yamada et al., 2000), and prepro-orexin KO mice and orexin KO mice are hypophagic compared to WT mice (Hara et al., 2001; Willie et al., 2001). Orexin neurons receive innervation from NPY/AgRP and α-MSH immunoreactive fibers (Broberger et al., 1998; Elias et al., 1998). Central administration of AgRP results in increased c-Fos expression in orexin but not MCH neurons of the lateral hypothalamus (Zheng et al., 2002). These findings collectively suggest that orexin has an important role in the regulation of feeding behavior. Lastly, the majority of orexin neurons are glutamatergic (Rosin et al., 2003; Torrealba et al., 2003) and not GABAergic (Rosin et al., 2003) although we did not assess these transmitters in this analysis.

Activation of PKCs has been demonstrated to cause desensitization of receptors (Huganir and Greengard, 1990), glutamate-induced neurotoxicity (Felipo et al., 1993), and neuropeptide release (Liu et al., 1992). PKC activation is downstream of G-protein coupled receptors (GPCRs), and orexin neurons may express GPCRs involved in feeding behavior, including Y4 receptors (Campbell et al., 2003), Y5 receptors (Gerald et al., 1996), melanocortin-4-receptors (MC4R) (Huszar et al., 1997), and orexin autoreceptors (Shiraishi et al., 2000). Hence, we hypothesize that activation of GPCR, by their respective agonists such as pancreatic polypeptide, NPY, AgRP or orexin, leads to coupling with excitatory G protein $G_{q/11}$. This activation presumably leads to agonist-induced hydrolysis of inositol phospholipids by phospholipase C (PLC) and results in an increase of DAG; and potentially activation of PKC-θ resulting in translocation to neuronal membranes where PKC-θ causes phosphorylation of calcium (Ca^{2+}) channels, leading to influx of Ca^{2+}, membrane depolarization, and potentially release of orexin, dynorphin and/or glutamate.

Other mechanisms by which PKC-θ may regulate orexin and glutamate release include phosphorylation-dependent inhibition of K^+ channels (Hermans and Challiss, 2001) and phosphorylation of a conserved threonine residue (T180) of the Kir6.2 subunit of the potassium dependent ATP (K_{ATP}) channel (Light et al., 2000), therefore increasing the effects of orexin. Lastly, orexin released from LHA orexin neurons may control feeding by acting on ARC NPY/AgRP (Horvath et al., 1999; Yamanaka et al., 2000), VMN and/or PVN neurons (Marcus et al., 2001). Here we observed moderate innervation of the ARC and VMN by PKC-θ immunoreactive fibers, whereas the PVN had dense innervation of PKC-θ immunoreactive fibers, some of which are colocalized with orexin fibers. These data further suggest a potential role for PKC-θ in modulating the hypothalamic NPY/AgRP-orexin feeding circuit.

Arousal—Orexin also regulates sleep/wake cycles (Chemelli et al., 1999; Lin et al., 1999). The tuberomammillary nucleus contains a high percentage of histaminergic neurons, heavily expresses orexin receptor 2 (OX2R) mRNA (Marcus et al., 2001), and receives dense orexin innervation (Chemelli et al., 1999; Lin et al., 1999; Torrealba et al., 2003). In addition, at least 90% of orexin-IR terminals in the tuberomammillary nucleus are glutamatergic (Torrealba et al., 2003). Importantly, we found PKC-θ immunoreactivity in areas surrounding the dorsal tuberomammillary nucleus and apparent innervations of VTM

histaminergic neurons by PKC-θ immunoreactive fibers. One model in which PKC-θ may modulate histamine release is through a $G_{q/11}$-PKC-θ mechanism via activation of Ca^{2+} channels. Another mechanism by which PKC-θ may modulate tuberomammillary nucleus neuronal function is through glutamate activation of group I metabotropic glutamate receptors (mGluIR) which are coupled with $G_{q/11}$ proteins. PKC-θ activation of mGluIR (Hermans and Challiss, 2001) may result in inhibition of K^+ or activation of Ca^{2+} channels leading to membrane depolarization and histamine release. Prolonged or repeated exposure of mGluIR to glutamate may result in desensitization of the receptor by phosphorylation of mGluIR by PKC-θ and hence prevent glutamate excitotoxicity in these neurons (Alaluf et al., 1995). Therefore, orexin and glutamatergic innervation to the tuberomammillary nucleus histaminergic neurons (presumably modulated by PKC-θ) may regulate feeding-related excitatory input neurons and may promote arousal in anticipation of feeding time.

Functional implications: PKC-θ in non-orexin neurons

We also observed a high concentration of PKC-θ-IR neurons in the medial habenular nucleus. The MHb has been implicated in regulating various behaviors including sleep and circadian rhythms (Haun et al., 1992; Zhao and Rusak, 2005). Importantly, the MHb contains high levels of $GABA_B$ receptors and MHb neurons are inhibited by GABA (Wang et al., 2006; Kim and Chung, 2007). The MHb innervates the interpenduncular nucleus (IPN), and these projections are known to be glutamatergic (Qin and Luo, 2009). Our results indicate a moderate distribution of PKC-θ-IR fibers in the IPN and surrounding midbrain nuclei. Therefore, one possibility is that PKC-θ may modulate glutamate release from MHb neurons.

We also observed moderate density PKC-θ-IR fibers in the VTA. These immunoreactive fibers were in close proximity with the orexin immunoreactive fibers. However, we found no colocalization with orexin fibers, suggesting that PKC-θ-IR fibers in the VTA may have originated from non-orexin neurons, such as neuronal populations in the MHb or tuberomammillary nucleus.

Functional implications: PKC-δ in oxytocin neurons

Oxytocin is involved in lactation, feeding and sexual behavior (Gimpl and Fahrenholz, 2001). In the brain, oxytocin is mainly synthesized in the magnocellular neurons of the PVN and SON (Silverman and Zimmerman, 1983). The bulk of the peptide is transported to the posterior pituitary via the internal zone of the median eminence (Wiegand and Price, 1980; Smith and Armstrong, 1990). In contrast, oxytocin neurons in the parvocellular subdivision of the PVN project to other brain regions such as the NTS and subfornical organ (Sawchenko and Swanson, 1982). Importantly, our findings indicate a high degree of colocalization of PKC-δ immunoreactivity in the PVN and SON oxytocin neurons, suggesting that PKC-δ may be an important modulator of oxytocin release. Furthermore, we also observed a dense innervation of PKC-δ fibers in the median eminence. No immunoreactive fibers were observed in the rest of the brain, with the exception of the lateral septal nucleus and suprachiasmatic nucleus. These results suggest that PKC-δ may be involved in modulation of oxytocin release to the posterior pituitary but not to other brain nuclei.

Hypothalamic oxytocin neurons receive dense glutamatergic innervation (van den Pol et al., 1990) and glutamate can regulate hypothalamic oxytocin release through activation of mGluIR (Pampillo et al., 2001). Importantly, PVN and SON magnocellular neurons have been demonstrated to express mGluIR (Meeker et al., 1994), and activation of mGluIR has been demonstrated to reduce K^+ currents in SON magnocellular neurons (Schrader and Tasker, 1997). Furthermore, activation of mGluIR participates in the stimulatory effects of glutamate on hypothalamic oxytocin release (Pampillo et al., 2001). As previously discussed, we hypothesize PKC-δ may modulate glutamate-dependent oxytocin release in a similar fashion, through mGluIR-$G_{q/11}$ dependent K^+ or Ca^{2+} channel phosphorylation. Lastly, oxytocin neurons also produce several other neuropeptides such as galanin (Skofitsch and Jacobowitz, 1986), and it is possible PKC-δ may regulate the release of these peptides as well.

CONCLUSION

Here we demonstrate PKC-θ and -δ neuronal distribution and their projections in the mouse and rat hypothalamus. We confirmed the presence of PKC-δ in several non-hypothalamic sites (Merchenthaler et al., 1993; Naik et al., 2000) and PKC-θ immunoreactivity in the ARC (Dewing et al., 2008; Benoit et al., 2009). We further found PKC-θ in hypothalamic orexin neurons and histamine-containing tuberomammillary neurons, suggesting that PKC-θ may be an important modulator of feeding behavior in these neuronal populations. Additionally, the distribution of PKC-δ in PVN and SON oxytocin neurons suggests a role for PKC-δ in regulating feeding, lactation and/or other neuroendocrine functions. Importantly, even though these novel PKC isoforms are found in different hypothalamic neuronal populations, they may have a common mechanism by which they modulate neuropeptide release. Future research will be required to determine the specific contribution of these two PKC isoforms in regulating hypothalamic neuroendocrine functions.

Acknowledgments

We would like to thank Dr. Martin Myers Jr. for providing us the LepR-b-EGFP mice, Dr. Masashi Yanagisawa for providing us the ORX-GFP mice. We would also like to thank Dr. Tom Finger and the Rocky Mountain Taste and Smell Center at the University of Colorado Denver for assistance with isolation of the PKC-δ KO mouse brains. This research was supported in part by NIH DK 17844 (DJC), NIH HD 061539 (CFE) and the American Heart Association (BGI).

Abbreviations

α-MSH	α-melanocyte stimulating hormone
ARC	arcuate hypothalamic nucleus
AVP	arginine vasopressin
DAG	diacylglycerol
EYFP	enhanced yellow fluorescent protein
GFP	green fluorescent protein

IPF	interpeduncular fossa
LepR-b	long form of leptin receptor
LHA	lateral hypothalamic area
MHb	medial habenular nucleus
MM	medial mammillary nucleus
ORX	orexin
Oxt	oxytocin
Pfx	perifornical area
PKC	protein kinase C
PKC-δ	PKC-delta
PKC-θ	PKC-theta
POMC	proopiomelanocortin
PVN	paraventricular hypothalamic nucleus
PVT	paraventricular thalamic nucleus
SON	supraoptic nucleus
vDMN	ventral part of the dorsomedial hypothalamic nucleus
VMN	ventromedial hypothalamic nucleus
VPL	ventral posterolateral thalamic nuclei
VPM	ventral posteromedial thalamic nuclei
VTA	ventral tegmental area
3v	third ventricle

References

Adamantidis A, de Lecea L. Physiological arousal: a role for hypothalamic systems. Cell Mol Life Sci. 2008; 65:1475–1488. [PubMed: 18351292]

Alaluf S, Mulvihill ER, McIlhinney RA. Rapid agonist mediated phosphorylation of the metabotropic glutamate receptor 1 alpha by protein kinase C in permanently transfected BHK cells. FEBS Lett. 1995; 367:301–305. [PubMed: 7607328]

Anand BK, Brobeck JR. Localization of a “feeding center” in the hypothalamus of the rat. Proc Soc Exp Biol Med. 1951; 77:323–324. [PubMed: 14854036]

Anand BK, Chhina GS, Sharma KN, Dua S, Singh B. Activity of single neurons in the hypothalamic feeding centers: effect of glucose. Am J Physiol. 1964; 207:1146–1154. [PubMed: 14237464]

Balthasar N, Dalgaard LT, Lee CE, Yu J, Funahashi H, Williams T, Ferreira M, Tang V, McGovern RA, Kenny CD, Christiansen LM, Edelstein E, Choi B, Boss O, Aschkenasi C, Zhang CY, Mountjoy K,

Kishi T, Elmquist JK, Lowell BB. Divergence of melanocortin pathways in the control of food intake and energy expenditure. Cell. 2005; 123:493–505. [PubMed: 16269339]

Benoit SC, Kemp CJ, Elias CF, Abplanalp W, Herman JP, Migrenne S, Lefevre AL, Cruciani-Guglielmacci C, Magnan C, Yu F, Niswender K, Irani BG, Holland WL, Clegg DJ. Palmitic acid mediates hypothalamic insulin resistance by altering PKC-theta subcellular localization in rodents. J Clin Invest. 2009; 119:2577–2589. [PubMed: 19726875]

Broberger C, De Lecea L, Sutcliffe JG, Hokfelt T. Hypocretin/orexin- and melanin-concentrating hormone-expressing cells form distinct populations in the rodent lateral hypothalamus: relationship to the neuropeptide Y and agouti gene-related protein systems. J Comp Neurol. 1998; 402:460–474. [PubMed: 9862321]

Campbell RE, Smith MS, Allen SE, Grayson BE, Ffrench-Mullen JM, Grove KL. Orexin neurons express a functional pancreatic polypeptide Y4 receptor. J Neurosci. 2003; 23:1487–1497. [PubMed: 12598637]

Campenot RB, Draker DD, Senger DL. Evidence that protein kinase C activities involved in regulating neurite growth are localized to distal neurites. J Neurochem. 1994; 63:868–878. [PubMed: 7519663]

Chemelli RM, Willie JT, Sinton CM, Elmquist JK, Scammell T, Lee C, Richardson JA, Williams SC, Xiong Y, Kisanuki Y, Fitch TE, Nakazato M, Hammer RE, Saper CB, Yanagisawa M. Narcolepsy in orexin knockout mice: molecular genetics of sleep regulation. Cell. 1999; 98:437–451. [PubMed: 10481909]

Cheung CC, Clifton DK, Steiner RA. Proopiomelanocortin neurons are direct targets for leptin in the hypothalamus. Endocrinology. 1997; 138:4489–4492. [PubMed: 9322969]

Cowley MA, Smart JL, Rubinstein M, Cerdan MG, Diano S, Horvath TL, Cone RD, Low MJ. Leptin activates anorexigenic POMC neurons through a neural network in the arcuate nucleus. Nature. 2001; 411:480–484. [PubMed: 11373681]

Date Y, Ueta Y, Yamashita H, Yamaguchi H, Matsukura S, Kangawa K, Sakurai T, Yanagisawa M, Nakazato M. Orexins, orexigenic hypothalamic peptides, interact with autonomic, neuroendocrine and neuroregulatory systems. Proc Natl Acad Sci U S A. 1999; 96:748–753. [PubMed: 9892705]

Dewing P, Christensen A, Bondar G, Micevych P. Protein kinase C signaling in the hypothalamic arcuate nucleus regulates sexual receptivity in female rats. Endocrinology. 2008; 149:5934–5942. [PubMed: 18653714]

Elias CF, Saper CB, Maratos-Flier E, Tritos NA, Lee C, Kelly J, Tatro JB, Hoffman GE, Ollmann MM, Barsh GS, Sakurai T, Yanagisawa M, Elmquist JK. Chemically defined projections linking the mediobasal hypothalamus and the lateral hypothalamic area. J Comp Neurol. 1998; 402:442–459. [PubMed: 9862320]

Felipo V, Minana MD, Grisolia S. Inhibitors of protein kinase C prevent the toxicity of glutamate in primary neuronal cultures. Brain Res. 1993; 604:192–196. [PubMed: 7681344]

Gerald C, Walker MW, Criscione L, Gustafson EL, Batzl-Hartmann C, Smith KE, Vaysse P, Durkin MM, Laz TM, Linemeyer DL, Schaffhauser AO, Whitebread S, Hofbauer KG, Taber RI, Branchek TA, Weinshank RL. A receptor subtype involved in neuropeptide-Y-induced food intake. Nature. 1996; 382:168–171. [PubMed: 8700207]

Gimpl G, Fahrenholz F. The oxytocin receptor system: structure, function, and regulation. Physiol Rev. 2001; 81:629–683. [PubMed: 11274341]

Guillery RW, Herrup K. Quantification without pontification: choosing a method for counting objects in sectioned tissues. J Comp Neurol. 1997; 386:2–7. [PubMed: 9303520]

Hara J, Beuckmann CT, Nambu T, Willie JT, Chemelli RM, Sinton CM, Sugiyama F, Yagami K, Goto K, Yanagisawa M, Sakurai T. Genetic ablation of orexin neurons in mice results in narcolepsy, hypophagia, and obesity. Neuron. 2001; 30:345–354. [PubMed: 11394998]

Haun F, Eckenrode TC, Murray M. Habenula and thalamus cell transplants restore normal sleep behaviors disrupted by denervation of the interpeduncular nucleus. J Neurosci. 1992; 12:3282–3290. [PubMed: 1494957]

Haynes AC, Jackson B, Chapman H, Tadayyon M, Johns A, Porter RA, Arch JR. A selective orexin-1 receptor antagonist reduces food consumption in male and female rats. Regul Pept. 2000; 96:45–51. [PubMed: 11102651]

Hermans E, Challiss RA. Structural, signalling and regulatory properties of the group I metabotropic glutamate receptors: prototypic family C G-protein-coupled receptors. Biochem J. 2001; 359:465–484. [PubMed: 11672421]

Hill JW, Elmquist JK, Elias CF. Hypothalamic pathways linking energy balance and reproduction. Am J Physiol Endocrinol Metab. 2008; 294:E827–E832. [PubMed: 18285524]

Horvath TL, Diano S, van den Pol AN. Synaptic interaction between hypocretin (orexin) and neuropeptide Y cells in the rodent and primate hypothalamus: a novel circuit implicated in metabolic and endocrine regulations. J Neurosci. 1999; 19:1072–1087. [PubMed: 9920670]

Huganir RL, Greengard P. Regulation of neurotransmitter receptor desensitization by protein phosphorylation. Neuron. 1990; 5:555–567. [PubMed: 1699566]

Humphries MJ, Limesand KH, Schneider JC, Nakayama KI, Anderson SM, Reyland ME. Suppression of apoptosis in the protein kinase Cdelta null mouse *in vivo*. J Biol Chem. 2006; 281:9728–9737. [PubMed: 16452485]

Huszar D, Lynch CA, Fairchild-Huntress V, Dunmore JH, Fang Q, Berkemeier LR, Gu W, Kesterson RA, Boston BA, Cone RD, Smith FJ, Campfield LA, Burn P, Lee F. Targeted disruption of the melanocortin-4 receptor results in obesity in mice. Cell. 1997; 88:131–141. [PubMed: 9019399]

Kim U, Chung LY. Dual GABAergic synaptic response of fast excitation and slow inhibition in the medial habenula of rat epithalamus. J Neurophysiol. 2007; 98:1323–1332. [PubMed: 17615126]

Konno Y, Ohno S, Akita Y, Kawasaki H, Suzuki K. Enzymatic properties of a novel phorbol ester receptor/protein kinase, nPKC. J Biochem. 1989; 106:673–678. [PubMed: 2606915]

Lee EC, Yu D, Martinez de Velasco J, Tessarollo L, Swing DA, Court DL, Jenkins NA, Copeland NG. A highly efficient Escherichia coli-based chromosome engineering system adapted for recombinogenic targeting and subcloning of BAC DNA. Genomics. 2001; 73:56–65. [PubMed: 11352566]

Leinninger GM, Jo YH, Leshan RL, Louis GW, Yang H, Barrera JG, Wilson H, Opland DM, Faouzi MA, Gong Y, Jones JC, Rhodes CJ, Chua S Jr, Diano S, Horvath TL, Seeley RJ, Becker JB, Munzberg H, Myers MG Jr. Leptin acts via leptin receptor-expressing lateral hypothalamic neurons to modulate the mesolimbic dopamine system and suppress feeding. Cell Metab. 2009; 10:89–98. [PubMed: 19656487]

Leshan RL, Louis GW, Jo YH, Rhodes CJ, Munzberg H, Myers MG Jr. Direct innervation of GnRH neurons by metabolic- and sexual odorant-sensing leptin receptor neurons in the hypothalamic ventral premammillary nucleus. J Neurosci. 2009; 29:3138–3147. [PubMed: 19279251]

Li Y, Gao XB, Sakurai T, van den Pol AN. Hypocretin/Orexin excites hypocretin neurons via a local glutamate neuron-A potential mechanism for orchestrating the hypothalamic arousal system. Neuron. 2002; 36:1169–1181. [PubMed: 12495630]

Light PE, Bladen C, Winkfein RJ, Walsh MP, French RJ. Molecular basis of protein kinase C-induced activation of ATP-sensitive potassium channels. Proc Natl Acad Sci U S A. 2000; 97:9058–9063. [PubMed: 10908656]

Lin L, Faraco J, Li R, Kadotani H, Rogers W, Lin X, Qiu X, de Jong PJ, Nishino S, Mignot E. The sleep disorder canine narcolepsy is caused by a mutation in the hypocretin (orexin) receptor 2 gene. Cell. 1999; 98:365–376. [PubMed: 10458611]

Liu JP, Engler D, Funder JW, Robinson PJ. Evidence that the stimulation by arginine vasopressin of the release of adrenocorticotropin from the ovine anterior pituitary involves the activation of protein kinase C. Mol Cell Endocrinol. 1992; 87:35–47. [PubMed: 1332907]

Marcus JN, Aschkenasi CJ, Lee CE, Chemelli RM, Saper CB, Yanagisawa M, Elmquist JK. Differential expression of orexin receptors 1 and 2 in the rat brain. J Comp Neurol. 2001; 435:6–25. [PubMed: 11370008]

Marks JL, Porte D Jr, Stahl WL, Baskin DG. Localization of insulin receptor mRNA in rat brain by *in situ* hybridization. Endocrinology. 1990; 127:3234–3236. [PubMed: 2249648]

Meeker RB, Greenwood RS, Hayward JN. Glutamate receptors in the rat hypothalamus and pituitary. Endocrinology. 1994; 134:621–629. [PubMed: 7905409]

Mercer JG, Hoggard N, Williams LM, Lawrence CB, Hannah LT, Morgan PJ, Trayhurn P. Coexpression of leptin receptor and preproneuropeptide Y mRNA in arcuate nucleus of mouse hypothalamus. J Neuroendocrinol. 1996; 8:733–735. [PubMed: 8910801]

Merchenthaler I, Liposits Z, Reid JJ, Wetsel WC. Light and electron microscopic immunocytochemical localization of PKC delta immunoreactivity in the rat central nervous system. J Comp Neurol. 1993; 336:378–399. [PubMed: 8263228]

Minami H, Owada Y, Suzuki R, Handa Y, Kondo H. Localization of mRNAs for novel, atypical as well as conventional protein kinase C (PKC) isoforms in the brain of developing and mature rats. J Mol Neurosci. 2000; 15:121–135. [PubMed: 11220785]

Miyamoto A, Nakayama K, Imaki H, Hirose S, Jiang Y, Abe M, Tsukiyama T, Nagahama H, Ohno S, Hatakeyama S, Nakayama KI. Increased proliferation of B cells and auto-immunity in mice lacking protein kinase Cdelta. Nature. 2002; 416:865–869. [PubMed: 11976687]

Naik MU, Benedikz E, Hernandez I, Libien J, Hrabe J, Valsamis M, Dow-Edwards D, Osman M, Sacktor TC. Distribution of protein kinase Mzeta and the complete protein kinase C isoform family in rat brain. J Comp Neurol. 2000; 426:243–258. [PubMed: 10982466]

Nambu T, Sakurai T, Mizukami K, Hosoya Y, Yanagisawa M, Goto K. Distribution of orexin neurons in the adult rat brain. Brain Res. 1999; 827:243–260. [PubMed: 10320718]

Niswender KD, Schwartz MW. Insulin and leptin revisited: adiposity signals with overlapping physiological and intracellular signaling capabilities. Front Neuroendocrinol. 2003; 24:1–10. [PubMed: 12609497]

Ono Y, Fujii T, Ogita K, Kikkawa U, Igarashi K, Nishizuka Y. The structure, expression, and properties of additional members of the protein kinase C family. J Biol Chem. 1988; 263:6927–6932. [PubMed: 2834397]

Osada S, Mizuno K, Saido TC, Suzuki K, Kuroki T, Ohno S. A new member of the protein kinase C family, nPKC theta, predominantly expressed in skeletal muscle. Mol Cell Biol. 1992; 12:3930–3938. [PubMed: 1508194]

Pampillo M, del Carmen Diaz M, Duvilanski BH, Rettori V, Seilicovich A, Lasaga M. Differential effects of glutamate agonists and D-aspartate on oxytocin release from hypothalamus and posterior pituitary of male rats. Endocrine. 2001; 15:309–315. [PubMed: 11762705]

Paxinos, G.; Franklin, KBJ. The mouse brain in stereotaxic coordinates. 2. San Diego, CA: Academic Press; 2001.

Qin C, Luo M. Neurochemical phenotypes of the afferent and efferent projections of the mouse medial habenula. Neuroscience. 2009; 161:827–837. [PubMed: 19362132]

Rosin DL, Weston MC, Sevigny CP, Stornetta RL, Guyenet PG. Hypothalamic orexin (hypocretin) neurons express vesicular glutamate transporters VGLUT1 or VGLUT2. J Comp Neurol. 2003; 465:593–603. [PubMed: 12975818]

Ross R, Wang PY, Chari M, Lam CK, Caspi L, Ono H, Muse ED, Li X, Gutierrez-Juarez R, Light PE, Schwartz GJ, Rossetti L, Lam TK. Hypothalamic protein kinase C regulates glucose production. Diabetes. 2008; 57:2061–2065. [PubMed: 18511848]

Saito N, Itouji A, Totani Y, Osawa I, Koide H, Fujisawa N, Ogita K, Tanaka C. Cellular and intracellular localization of epsilon-subspecies of protein kinase C in the rat brain; presynaptic localization of the epsilon-subspecies. Brain Res. 1993; 607:241–248. [PubMed: 8481800]

Sakurai T, Amemiya A, Ishii M, Matsuzaki I, Chemelli RM, Tanaka H, Williams SC, Richardson JA, Kozlowski GP, Wilson S, Arch JR, Buckingham RE, Haynes AC, Carr SA, Annan RS, McNulty DE, Liu WS, Terrett JA, Elshourbagy NA, Bergsma DJ, Yanagisawa M. Orexins and orexin receptors: a family of hypothalamic neuropeptides and G protein-coupled receptors that regulate feeding behavior. Cell. 1998; 92:573–585. [PubMed: 9491897]

Sakurai T, Moriguchi T, Furuya K, Kajiwara N, Nakamura T, Yanagisawa M, Goto K. Structure and function of human prepro-orexin gene. J Biol Chem. 1999; 274:17771–17776. [PubMed: 10364220]

Sawchenko PE, Swanson LW. Immunohistochemical identification of neurons in the paraventricular nucleus of the hypothalamus that project to the medulla or to the spinal cord in the rat. J Comp Neurol. 1982; 205:260–272. [PubMed: 6122696]

Schrader LA, Tasker JG. Modulation of multiple potassium currents by metabotropic glutamate receptors in neurons of the hypothalamic supraoptic nucleus. J Neurophysiol. 1997; 78:3428–3437. [PubMed: 9405556]

Schwartz MW, Woods SC, Porte D Jr, Seeley RJ, Baskin DG. Central nervous system control of food intake. Nature. 2000; 404:661–671. [PubMed: 10766253]

Scott MM, Lachey JL, Sternson SM, Lee CE, Elias CF, Friedman JM, Elmquist JK. Leptin targets in the mouse brain. J Comp Neurol. 2009; 514:518–532. [PubMed: 19350671]

Shearman MS, Sekiguchi K, Nishizuka Y. Modulation of ion channel activity: a key function of the protein kinase C enzyme family. Pharmacol Rev. 1989; 41:211–237. [PubMed: 2481858]

Shiraishi T, Oomura Y, Sasaki K, Wayner MJ. Effects of leptin and orexin-A on food intake and feeding related hypothalamic neurons. Physiol Behav. 2000; 71:251–261. [PubMed: 11150556]

Silverman AJ, Zimmerman EA. Magnocellular neurosecretory system. Annu Rev Neurosci. 1983; 6:357–380. [PubMed: 6301350]

Skofitsch G, Jacobowitz DM. Quantitative distribution of galanin-like immunoreactivity in the rat central nervous system. Peptides. 1986; 7:609–613. [PubMed: 2429289]

Smith BN, Armstrong WE. Tuberal supraoptic neurons–I. Morphological and electrophysiological characteristics observed with intracellular recording and biocytin filling *in vitro*. Neuroscience. 1990; 38:469–483. [PubMed: 2124666]

Tanaka C, Nishizuka Y. The protein kinase C family for neuronal signaling. Annu Rev Neurosci. 1994; 17:551–567. [PubMed: 8210187]

Torrealba F, Yanagisawa M, Saper CB. Colocalization of orexin a and glutamate immunoreactivity in axon terminals in the tuberomammillary nucleus in rats. Neuroscience. 2003; 119:1033–1044. [PubMed: 12831862]

Tsujino N, Sakurai T. Orexin/Hypocretin: a neuropeptide at the interface of sleep, energy homeostasis, and reward system. Pharmacol Rev. 2009; 61:162–176. [PubMed: 19549926]

Ueta Y, Fujihara H, Serino R, Dayanithi G, Ozawa H, Matsuda K, Kawata M, Yamada J, Ueno S, Fukuda A, Murphy D. Transgenic expression of enhanced green fluorescent protein enables direct visualization for physiological studies of vasopressin neurons and isolated nerve terminals of the rat. Endocrinology. 2005; 146:406–413. [PubMed: 15375027]

van den Pol AN, Wuarin JP, Dudek FE. Glutamate, the dominant excitatory transmitter in neuroendocrine regulation. Science. 1990; 250:1276–1278. [PubMed: 1978759]

van den Top M, Lee K, Whyment AD, Blanks AM, Spanswick D. Orexigen-sensitive NPY/AgRP pacemaker neurons in the hypothalamic arcuate nucleus. Nat Neurosci. 2004; 7:493–494. [PubMed: 15097991]

Wang DG, Gong N, Luo B, Xu TL. Absence of GABA type A signaling in adult medial habenular neurons. Neuroscience. 2006; 141:133–141. [PubMed: 16675141]

Wetsel WC, Khan WA, Merchenthaler I, Rivera H, Halpern AE, Phung HM, Negro-Vilar A, Hannun YA. Tissue and cellular distribution of the extended family of protein kinase C isoenzymes. J Cell Biol. 1992; 117:121–133. [PubMed: 1556149]

Wiegand SJ, Price JL. Cells of origin of the afferent fibers to the median eminence in the rat. J Comp Neurol. 1980; 192:1–19. [PubMed: 7410605]

Willie JT, Chemelli RM, Sinton CM, Yanagisawa M. To eat or to sleep? Orexin in the regulation of feeding and wakefulness. Annu Rev Neurosci. 2001; 24:429–458. [PubMed: 11283317]

Yamada H, Okumura T, Motomura W, Kobayashi Y, Kohgo Y. Inhibition of food intake by central injection of anti-orexin antibody in fasted rats. Biochem Biophys Res Commun. 2000; 267:527–531. [PubMed: 10631095]

Yamanaka A, Beuckmann CT, Willie JT, Hara J, Tsujino N, Mieda M, Tominaga M, Yagami K, Sugiyama F, Goto K, Yanagisawa M, Sakurai T. Hypothalamic orexin neurons regulate arousal according to energy balance in mice. Neuron. 2003; 38:701–713. [PubMed: 12797956]

Yamanaka A, Kunii K, Nambu T, Tsujino N, Sakai A, Matsuzaki I, Miwa Y, Goto K, Sakurai T. Orexin-induced food intake involves neuropeptide Y pathway. Brain Res. 2000; 859:404–409. [PubMed: 10719096]

Zhao CM, Furnes MW, Stenstrom B, Kulseng B, Chen D. Characterization of obestatin- and ghrelin-producing cells in the gastrointestinal tract and pancreas of rats: an immunohistochemical and electron-microscopic study. Cell Tissue Res. 2008a; 331:575–587. [PubMed: 18071756]

Zhao H, Rusak B. Circadian firing-rate rhythms and light responses of rat habenular nucleus neurons *in vivo* and *in vitro*. Neuroscience. 2005; 132:519–528. [PubMed: 15802202]

Zhao Y, Flandin P, Long JE, Cuesta MD, Westphal H, Rubenstein JL. Distinct molecular pathways for development of telencephalic interneuron subtypes revealed through analysis of Lhx6 mutants. J Comp Neurol. 2008b; 510:79–99. [PubMed: 18613121]

Zheng H, Corkern MM, Crousillac SM, Patterson LM, Phifer CB, Berthoud HR. Neurochemical phenotype of hypothalamic neurons showing Fos expression 23 h after intracranial AgRP. Am J Physiol Regul Integr Comp Physiol. 2002; 282:R1773–R1781. [PubMed: 12010760]

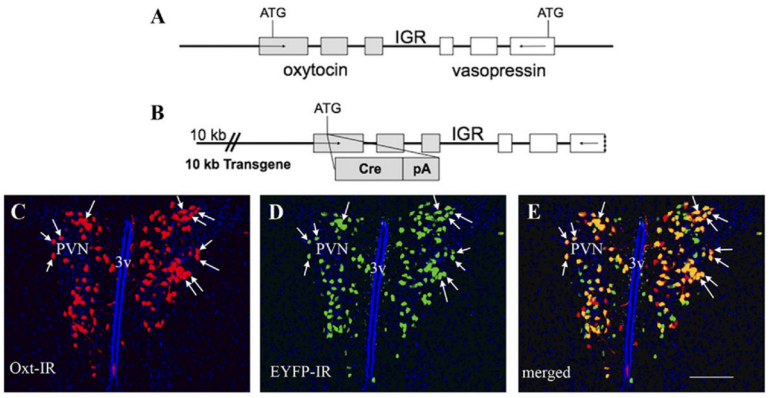

Fig. 1.

Generation of the Oxt-Cre mice. (A) Map of mouse oxytocin/vasopressin locus. (B) Transgene with Cre recombinase inserted into *Oxt* gene and vasopressin ATG codon mutated. Double label IHC for: oxytocin neurons (C) and EYFP (D) showed a high degree of colocalization (E). Colocalized neurons are indicated with white arrows. Scale bar=200 μm for (C–E). IGR, intergenic region.

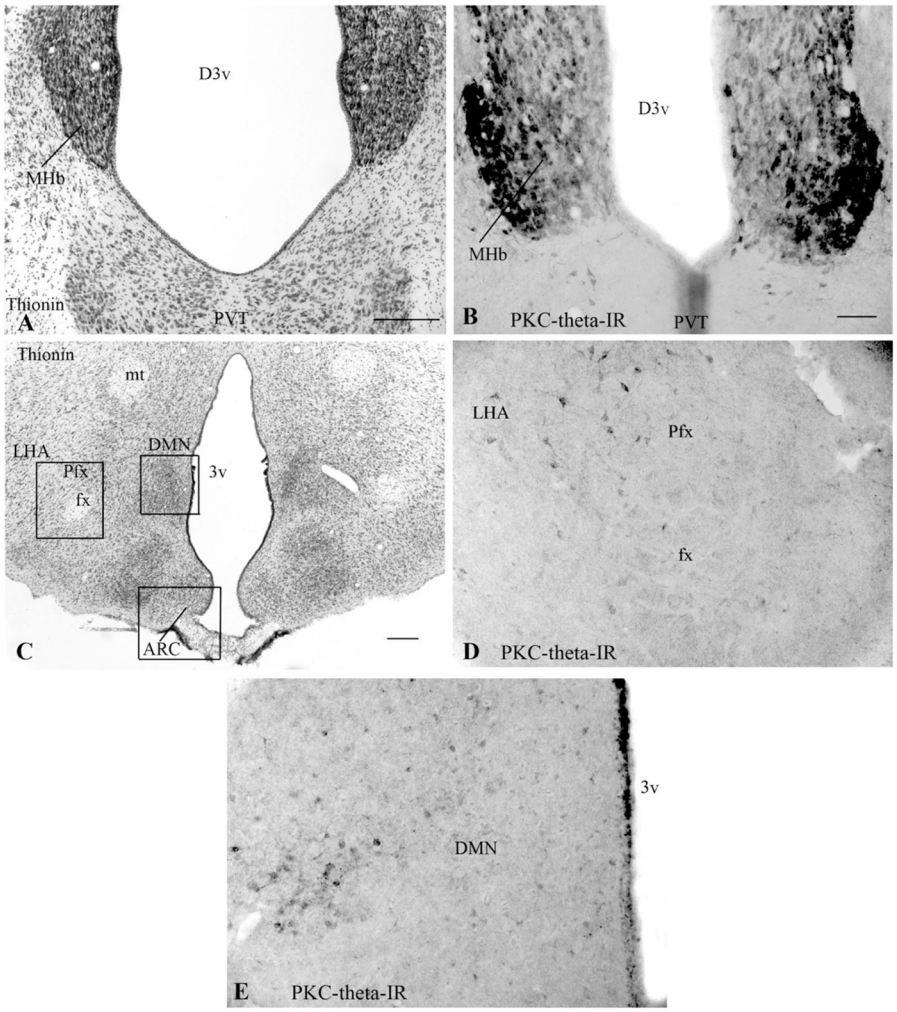

Fig. 2.

Distribution of PKC-*θ*-IR neurons in rat brain. (A) Thionin-stained section denoting the thalamic nuclei (MHb and PVT) of the brain. (B) Adjacent section of the brain shown in (A), showing PKC-*θ*-IR neurons in the MHb and PVT. (C) Low-power magnification of a thionin-stained section of hypothalamic nuclei. (D) PKC-*θ*-IR neurons in the LHA and Pfx. (E) PKC-*θ*-IR neurons in the DMN. 3v, third ventricle; ARC, arcuate hypothalamic nucleus; D3v, dorsal third ventricle; DMN, dorsomedial hypothalamic nucleus; fx, fornix; LHA, lateral hypothalamic area; MHb, medial habenular nucleus; mt, mammillothalamic tract; Pfx, perifornical area; PVT, paraventricular thalamic nucleus. Scale bars=200 *μ*m for (A); 50 *μ*m for (B, D, E); 100 *μ*m for (C).

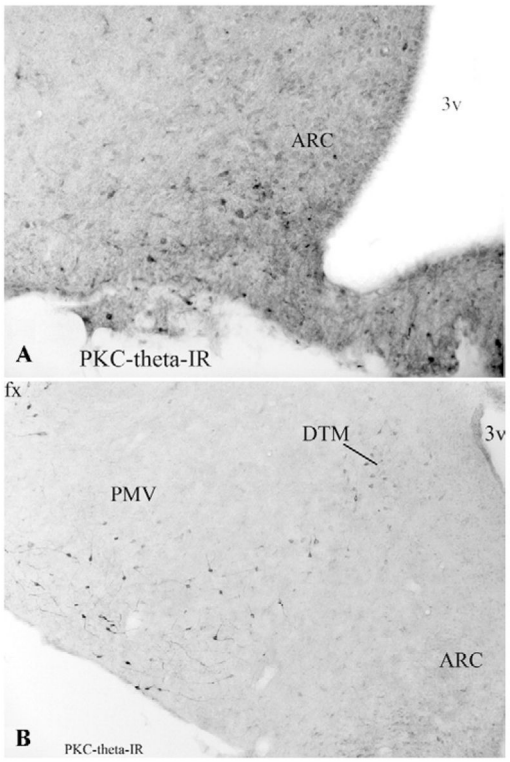

Fig. 3.

Distribution of PKC-*θ*-IR neurons in the rat hypothalamic arcuate nucleus (ARC). (A) PKC-*θ*-IR neurons in the ARC. (B) PKC-*θ*-IR neurons in the DTM and in ventral aspects of the PMV. 3v, third ventricle; DTM, dorsal tuberomammillary nucleus; fx, fornix; PMV, ventral premammillary nucleus. Scale bars=100 μm for (A, B).

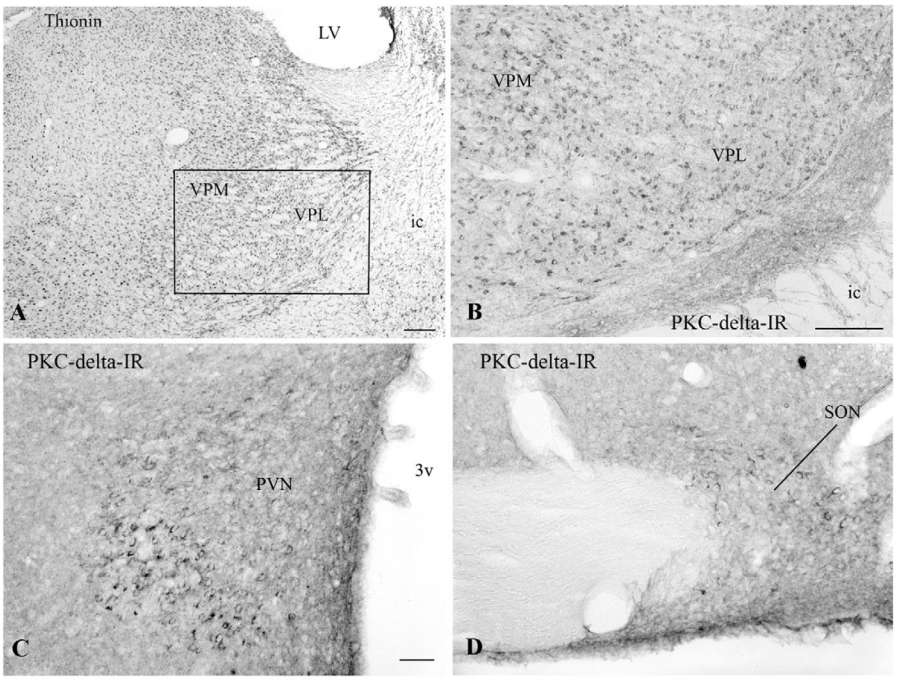

Fig. 4.

Distribution of PKC-δ-IR neurons in rat brain. (A) Thionin-stained section denoting the thalamic nuclei (VPM and VPL) of the brain. (B) Adjacent section of the brain shown in (A) at higher magnification, showing PKC-δ-IR neurons in the VPM and VPL. (C) PKC-δ-IR neurons in the PVN. (D) PKC-δ-IR neurons in the SON. 3v, third ventricle; fx, fornix; ic, internal capsule; LV, lateral ventricle; PVN, paraventricular hypothalamic nucleus; SON, supraoptic nucleus; VPL, ventral posterolateral thalamic nucleus; VPM, ventral posteromedial thalamic nucleus. Scale bars=200 μm for (A); 200 μm for (B); 50 μm for (C, D).

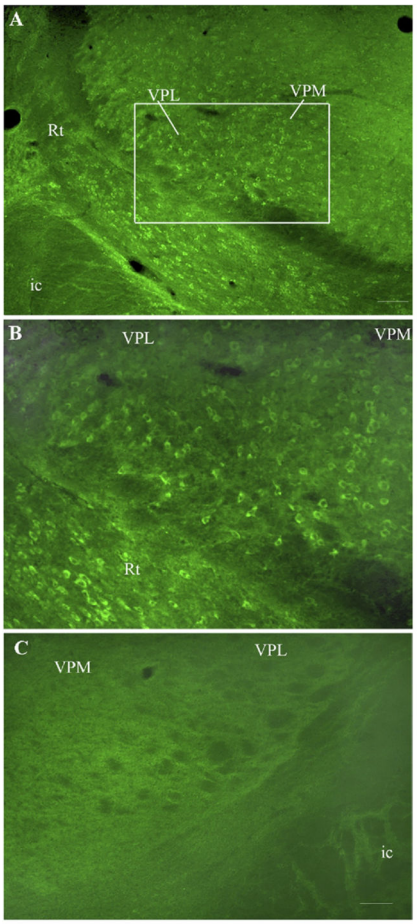

Fig. 5.

Validation of PKC-δ antibody. (A) Low power magnification of PKC-δ fluorescent IHC in the thalamic nuclei (VPM and VPL) of the mouse brain. (B) Higher power view of boxed area in (A). (C) Lack of staining in section from same atlas level as (B) in PKC-δ-KO mouse. ic, internal capsule; Rt, reticular thalamic nucleus; VPL, ventral posterolateral thalamic nucleus; VPM, ventral posteromedial thalamic nucleus. Scale bars=100 μm for (A); (B, C)=50 μm.

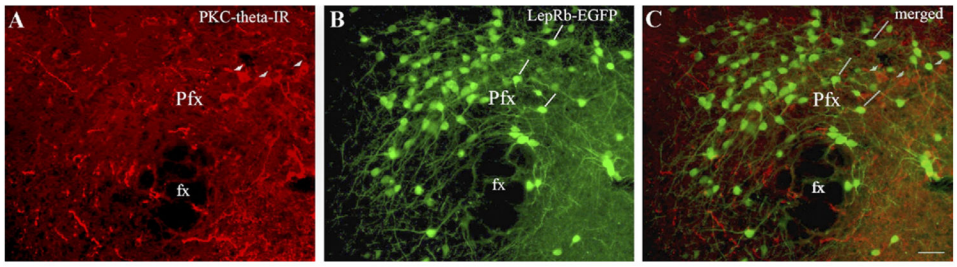

Fig. 6.

Double-label IHC for PKC-*θ*-IR neurons (A, denoted by white arrow heads) and LepR-b-EGFP in mouse hypothalamus (B, denoted by white lines) showed no colocalization (C) in the Pfx. fx, fornix; Pfx, perifornical area. Scale bar=50 μm for (A–C).

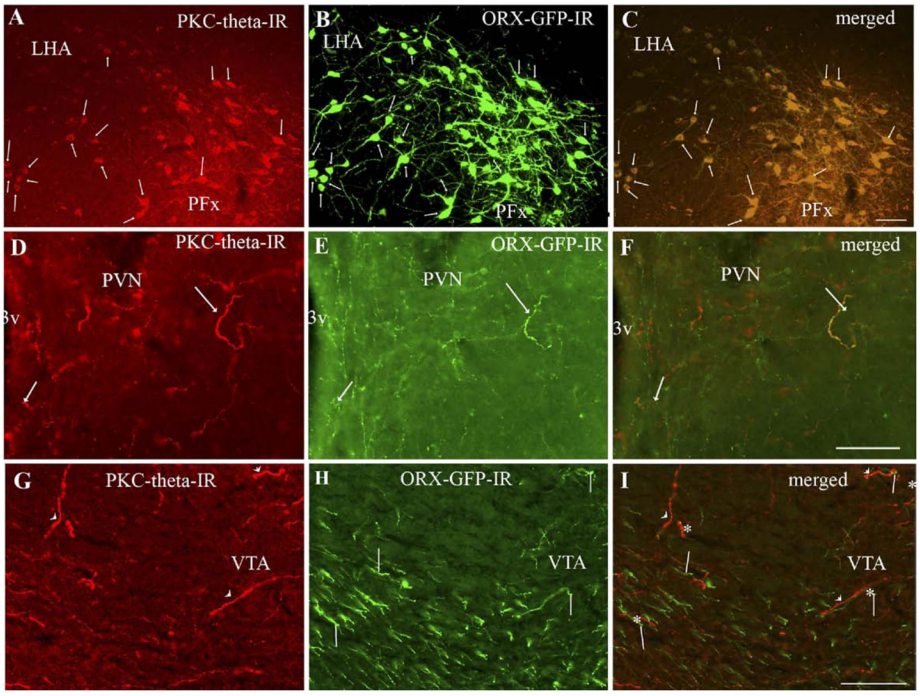

Fig. 7.

Double label IHC for: PKC-*θ*-IR neurons (A) and ORX-GFP (B) in mouse hypothalamus showed a high degree of colocalization (C). Colocalized neurons are indicated with white arrows. High density of PKC-*θ*-IR (D) and ORX-GFP-IR fibers (E) in the PVN. Overlapping PKC-*θ*-IR and ORX-GFP-IR fibers (F, denoted by white arrows). High density of PKC-*θ*-IR (G) and ORX-GFP-IR fibers (H) in the VTA. No overlapping distribution pattern of PKC-*θ*-IR (denoted by white arrowheads) and ORX-GFP-IR fibers were observed (I). The fibers lay adjacent to each other and made several appositions. Points where appositions are made have been indicated by *. 3v, third ventricle; IPF, interpeduncular fossa; LHA, lateral hypothalamic area; MM, medial mammillary nucleus; Pfx, perifornical area; PVN, paraventricular hypothalamic nucleus; VTA, ventral tegmental area. Scale bars=50 μm for (A–C); 100 μm for (D–F); 100 μm for (G–I).

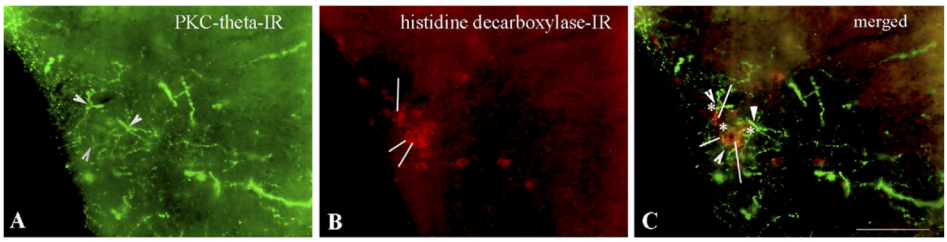

Fig. 8.

Double label IHC for: PKC-*θ*-IR (A, denoted by white arrow heads) and histidine decarboxylase-IR (B, denoted by white lines) in mouse hypothalamus showed several appositions (C). Points where appositions are made have been indicated by *. Scale bar=100 *μ*m.

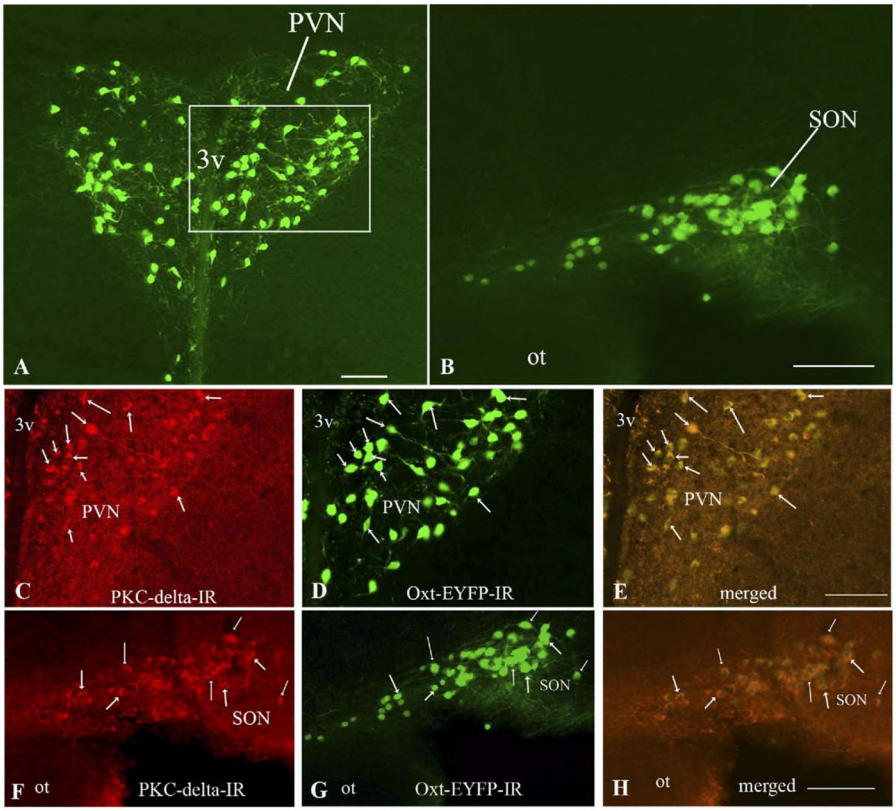

Fig. 9.

Colocalization between Oxt-YFP-IR and PKC-δ-IR neurons in the mouse hypothalamus. Lower power magnification of Oxt-YFP-IR neurons in PVN (A) and SON (B). Double-label IHC for PKC-δ-IR (C) and Oxt-YFP-IR (D) in boxed area of (A) showed a high degree of colocalization in the PVN (E). Double-label IHC for PKC-δ-IR (F) and Oxt-YFP-IR (G) showed a moderate degree of colocalization in the SON (H). Examples of colocalized neurons are indicated by white arrows. 3v, third ventricle; PVN, paraventricular hypothalamic nucleus; SON, supraoptic nucleus. Scale bars=100 μm for (A–G).

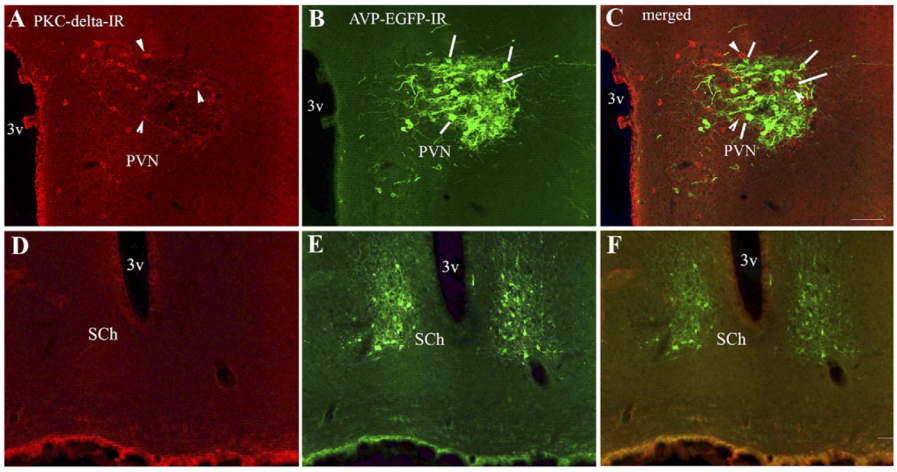

Fig. 10.

Colocalization between PKC-δ-IR and AVP-IR in mouse hypothalamus. Double-label IHC for PKC-δ-IR neurons (A, denoted by white arrow heads) and AVP-EGFP in mouse hypothalamus (B, denoted by white lines) showed no colocalization (C) in the PVN. There was no PKC-δ-IR at this level of the SCh (D), only AVP-EGFP was observed (E) and hence no colocalization was observed (F). 3v, third ventricle; PVN, paraventricular hypothalamic nucleus; SCh, suprachiasmatic nucleus. Scale bars=100 μm for (A–C); 50 μm for (D–F).

Table 1

Distribution pattern of PKC-theta versus PKC-delta in the mouse brain

Brain area	PKC-θ-IR cells	PKC-δ-IR cells	PKC-θ-IR fibers	PKC-δ-IR fibers
Cerebral cortex				
Piriform cortex	−	−	+	−
Primary somatosensory cortex, forelimb region	−	−	+	−
Primary somatosensory cortex, hindlimb region	−	−	+	−
Amygdala				
Anterior amygdaloid area, dorsal	−	+++	−	−
Anterior amygdaloid area, ventral	−	++	−	−
Hippocampus and septum				
Dentate gyrus	−	+	−	−
CA1 field	−	+	−	−
CA3 field	−	++	−	−
Lateral septal nucleus	−	++	+	++
Thalamus				
Paraventricular thalamic nucleus	+	−	++	−
Medial habenular nucleus	+++	−	−	−
Lateral habenular nucleus	+	−	+	−
Reticular thalamic nucleus	−	+++	−	−
Ventral posterolateral thalamic nucleus	−	+++	−	−
Ventral posteromedial thalamic nucleus	−	+++	−	−
Ventrolateral thalamic nucleus	−	++	−	−
Ventromedial thalamic nucleus	−	++	−	−
Hypothalamic nuclei				
Medial preoptic nucleus	−	−	++	++
Medial forebrain bundle	−	−	++	++
Supraoptic nucleus	−	+++	−	−
Suprachiasmatic nucleus, dorsal	−	++	−	−
Anterior hypothalamic area	−	+	+++	−
Paraventricular hypothalamic nucleus	−	+++	+++	+
Perifornical area	+++	−	+++	−
Lateral hypothalamic area	+++	−	+++	−
Dorsomedial hypothalamic nucleus, ventral	++	−	++	−
Ventromedial hypothalamic nucleus	−	−	++	−
Median eminence	−	−	−	+++
Arcuate hypothalamic nucleus	++	−	++	−
Posterior hypothalamic area	−	−	++	−
Ventral premamillary nucleus	+	−	+	−
Ventral tuberomammillary nucleus	+	−	++	−
Dorsal tuberomammillary nucleus	++	−	−	−
Medial mamillary nucleus	−	−	++	−

Brain area	PKC-θ-IR cells	PKC-δ-IR cells	PKC-θ-IR fibers	PKC-δ-IR fibers
Supramammillary nucleus	−	−	++	−
Midbrain, pons and medulla oblongata				
Dorsal raphe	−	−	++	−
Interpenduncular nucleus	−	−	++	−
Periaqueductal gray matter	−	−	++	−
Substantia nigra, pars compacta	−	−	++	−
Ventral tegmental area	−	−	+++	−
Nucleus of the solitary tract	−	−	+	−

Qualitative estimates of number of labeled PKC-θ and -δ cells and immunoreactive fibers. The following four point density scale was used: +++, high density; ++, moderate density; +, low density; −, absent.

Table 2

Double-labeled (PKC-θ+Orexin) neurons in mouse hypothalamic nuclei

Regions	Total PKC-θ	Total orexin	Doubles	% Doubles/total PKC-θ	% Doubles/total orexin
LHA	56±5.69	52±5.86	45.7±4.17	82.8±8.57	88.4±3.53
vDMN	11.3±0.88	9.33±1.15	9±0.58	84.2±11.6	96.7±3.33
Pfx	15.7±2.33	13.7±2.19	13.7±2.33	86.7±1.92	97±3.03

Values represent estimates of mean counts of cells±SEM (n=3). All cells were counted from atlas level 46 of Paxinos and Franklin (2001, 2nd Edition) Mouse Brain Atlas. LHA, lateral hypothalamic area; vDMN, ventral part of the dorsomedial hypothalamic nucleus.

Table 3

Double-labeled (PKC-δ+Oxytocin) neurons in mouse hypothalamic nuclei

Regions	Total PKC-δ	Total oxytocin	Doubles	% Doubles/total PKC-δ	% Doubles/total oxytocin
PVN	51.7±5.24	66±5.13	43.3±5.61	83.4±2.87	65.3±4.43
SON	20.67±1.2	34.7±2.91	17.3±0.33	84.5±5.28	50.7±4.24

Values represent estimates of mean counts of cells±SEM (*n*=3). All cells were counted from atlas level 38 of Paxinos and Franklin (2001, 2nd Edition) Mouse Brain Atlas. PVN, paraventricular hypothalamic nucleus; SON, supraoptic nucleus.